Published in final edited form as:
Biol Psychiatry. 2006 August 1; 60(3): 253–264. doi:10.1016/j.biopsych.2006.01.003.

A Neurobehavioral Systems Analysis of Adult Rats Exposed to Methylazoxymethanol Acetate on E17: Implications for the Neuropathology of Schizophrenia

Holly Moore, **J. David Jentsch**, **Mehdi Ghajarnia**, **Mark A. Geyer**, and **Anthony A. Grace**
Departments of Neuroscience, Psychiatry and Psychology (HM, JDJ, MG, AAG), University of Pittsburgh, Pittsburgh, Pennsylvania; and Department of Psychiatry (MAG), University of California, San Diego, San Diego, California.

Abstract

Background—As a test of plausibility for the hypothesis that schizophrenia can result from abnormal brain, especially cerebral cortical, development, these studies examined whether, in the rat, disruption of brain development initiated on embryonic day (E) 17, using the methylating agent methylazoxymethanol acetate (MAM), leads to a schizophrenia-relevant pattern of neural and behavioral pathology. Specifically, we tested whether this manipulation leads to disruptions of frontal and limbic corticostriatal circuit function, while producing schizophrenia-like, region-dependent reductions in gray matter in cortex and thalamus.

Methods—In offspring of rats administered MAM (22 mg/kg) on E17 or earlier (E15), regional size, neuron number and neuron density were determined in multiple brain regions. Spontaneous synaptic activity at prefrontal cortical (PFC) and ventral striatal (vSTR) neurons was recorded in vivio. Finally, cognitive and sensorimotor processes mediated by frontal and limbic corticostriatal circuits were assessed.

Results—Adult MAM-E17-exposed offspring showed selective histopathology: size reductions in mediodorsal thalamus, hippocampus, and parahippocampal, prefrontal, and occipital cortices, but not in sensory midbrain, cerebellum, or sensorimotor cortex. The prefrontal, perirhinal, and occipital cortices showed increased neuron density with no neuron loss. The histopathology was accompanied by a disruption of synaptically-driven “bistable membrane states” in PFC and vSTR neurons, and, at the behavioral level, cognitive inflexibility, orofacial dyskinesias, sensorimotor gating deficits and a post-pubertal-emerging hyper-responsiveness to amphetamine. Earlier embryonic MAM exposure led to microcephaly and a motor phenotype.

Conclusions—The “MAM-E17” rodent models key aspects of neuropathology in circuits that are highly relevant to schizophrenia.

Address reprint requests to Holly Moore, Ph.D., Columbia University, Department of Psychiatry, 1051 Riverside Dr, Mail Unit 14, New York, NY 10032; hm2035@columbia.edu..

Portions of these experiments have been reported in preliminary form at the Society for Neuroscience Annual Meeting 1997, New Orleans, Louisiana, October 25–30; the Society for Neuroscience Annual Meeting 1998, Los Angeles, California, November 7–12; the Society for Neuroscience Annual Meeting 1999, Miami Beach, Florida, October 23–28; and the Society for Neuroscience Annual Meeting 2002, Orlando, Florida, November 2–7.

We thank Susan R. Sesack for advice on the stereology experiments. We also thank Mrs. Nicole Macmurdo, Mr. Brian Seigworth, Ms. Darlene Giracello. and Mrs. Christy Smolak for excellent technical assistance and Ms. Karin Krueger for editorial assistance. The Neuroscope physiology data acquisition and analysis system was created by Mr. Brian Lowry. We greatly appreciate comments on previous versions of this manuscript provided by Drs. Stan P. Floresco, Hank P. Jedema, Antonieta Lavin, and Susan R. Sesack.

JDJ is currently affiliated with the Department of Psychology, University of California, Los Angeles, California.

Keywords

Frontal cortex; hippocampus; sensorimotor gating; reversal learning; schizophrenia; amphetamine

It remains unresolved whether the diverse yet distinct neuropathological and behavioral abnormalities observed in schizophrenia patients result from one or multiple etiologies (Andreasen and Carpenter 1993; Tsuang et al 2000). Reduced size of the medial temporal lobe (including hippocampus and parahippocampal regions) and histological abnormalities in this region are reliable features of schizophrenia (Harrison 2004; Shenton et al 2001). However, decreases in other cortical regions and the medial dorsal thalamus are also often reported (Harrison 1999; Shenton et al 2001). Although neuron loss is reported in the thalamus (Thune and Pakkenberg 2000), there appears to be no net loss of neurons in the cerebral cortex; thus, decreased cortical thickness in schizophrenia is concomitant with increased neuronal density (Selemon et al 1995; Thune and Pakkenberg 2000). Moreover this increased neuronal density, interpreted as a decrease in neuropil, is observed in prefrontal and occipital regions but not in the ventral lateral frontal cortex (Selemon et al 2003).

It is widely postulated that abnormal development of limbic and frontal cortical circuits leads to a dysregulation of basal ganglia and dopamine systems in schizophrenia (Lewis and Levitt 2002; Marenco and Weinberger 2000; Moore et al 1999; Waddington et al 1999). Dysfunction of frontal and limbic corticostriatal systems is evident in a number of behavioral deficits in schizophrenia. One such abnormality is in sensorimotor gating (Geyer et al 2001), a process mediated by temporal lobe and dopaminergic inputs to the limbic basal ganglia (Swerdlow et al 1999). Schizophrenia patients also show neuropsychological and neurological “signs” of frontal cortical damage, including cognitive inflexibility (Elliott et al 1995) and increases in spontaneous orofacial dyskinesias (Waddington et al 1995). Moreover, metabolic abnormalities in the prefrontal and/or limbic temporal cortices and anatomically related thalamus and basal ganglia are often correlated with cognitive and other behavioral deficits in schizophrenia (Andreasen et al 1997; Bilder et al 1995; Seidman et al 2003). Psychosis, which emerges in adolescence or adulthood in the majority of schizophrenia patients, is associated with increased striatal dopamine transmission. Specifically, schizophrenia patients show an exaggerated increase in striatal dopamine transmission in response to amphetamine, and this correlates with psychotic symptoms (Laruelle 2000). Thus, the psychopathology of schizophrenia appears to be driven by dysfunction of frontal and limbic cortical circuits and the dopaminergic inputs to the striatum (Grace 1993).

Several rodent models, e.g., the neonatal hippocampal lesion and chronic phencyclidine models, exhibit frontal lobe abnormalities, sensorimotor gating deficits, and dopamine system dysregulation relevant to schizophrenia (Bertolino et al 2002; Hanlon and Sutherland 2000; Jentsch et al 2003; Lipska and Weinberger 2000; O’Donnell et al 2002). However, it is not known whether a disruption of cerebral cortical development can lead to the specific patterns of histopathology and the neurobehavioral dysfunction observed in schizophrenia. The present experiments examined whether the methylating agent methylazoxymethanol acetate (MAM) (Nagata and Matsumoto 1969) would be useful in creating such a model. Administration of MAM to a pregnant rat dam can potently and selectively disrupt embryonic brain development (Eriksdotter-Nilsson et al 1986; Haddad et al 1972). Exposure to MAM on or prior to E15 leads to abnormalities in corticocortical synaptic transmission (Chevassus-Au-Louis et al 1998), striatal hyperdopaminergia with increased responsiveness to psychostimulants (Archer et al 1988; Watanabe et al 1995), and cognitive and sensorimotor gating deficits (Mohammed et al 1986; Talamini et al 2000). While these

abnormalities are relevant to a number of developmental brain disorders (Cattabeni and Di Luca 1997; Chevassus-Au-Louis et al 1998; Coyle et al 1984), their validity for modeling schizophrenia is limited due to the microcephaly produced by MAM exposure on or before E15 (Dambska et al 1982; Jongen-Relo et al 2004; Kabat et al 1985; Singh 1980). To address this limitation, we administered MAM on E17 (Grace and Moore 1998; Moore et al 2001). At this stage, proliferation has peaked in many cortical regions and is nearly completed or paused in most subcortical and cerebellar regions (Bayer and Altman 1995). Thus, we predicted that MAM-E17 exposure would have a more selective effect on the cerebral cortex and particularly on the later developing paralimbic frontal and temporal cortices (Bayer and Altman 1995). Thus, in the present study, we examined the morphology of these regions in the MAM-E17 model. We also examined the morphology of the medial dorsal and midline thalamic nuclei due to their reciprocal connections with the paralimbic frontal cortex (Price 1995) and the pathology in this region in schizophrenia (Thune and Pakkenberg 2000). In relation to the histopathological profile of schizophrenia, the patterns of morphological abnormalities across these and other brain regions were characterized in offspring of rat dams exposed to MAM on E17 or E15. Given that cortical neuronal loss is not a feature of schizophrenia, cortical neuronal number and density were also quantified in the MAM-E17 model.

Since the initial proposal that MAM-E17 exposure might be a more relevant model for schizophrenia (Grace and Moore 1998; Moore et al 2001), cognitive deficits, as well as cortical and striatal dopamine abnormalities, have been reported in this model (Flagstad et al 2004; Gourevitch et al 2004; Moore et al 2001). The present experiments extended these findings by examining the function of schizophrenia-related corticostriatal circuits in the MAM-E17 model using neurophysiological and behavioral methods. Behaviorally, we evaluated the function of neural systems that have anatomical and functional homology with human temporal and medial prefrontal cortical circuits (Moser and Moser 1998; Remijnse et al 2005; Robbins 1996). Prepulse inhibition of startle was measured to test sensorimotor gating (see above) (Geyer et al 2001; Swerdlow et al 1999). Frontal cortical function was assessed with spontaneous and learned behaviors. Given that orofacial dyskinesias are a reliable correlate of frontal cortical lesions or dysfunction in rats (Gunne et al 1982) and humans (Waddington et al 1995), we measured spontaneous and N-methyl-D-aspartate (NMDA)-antagonist-induced orofacial dyskinesias in MAM-E17 offspring. The orbital and prelimbic/infralimbic regions of the prefrontal cortex mediate forms of reversal learning in the rat and human (Chudasama and Robbins 2003; Clark et al 2004; Kim and Ragozzino 2005). We hypothesized that, as with schizophrenia (Elliott et al 1995), functions of these regions, and thus reversal learning, would be impaired in the MAM-E17-offspring. Finally, we tested whether MAM-E17 exposure would lead to a developmentally delayed dysregulation of striatal dopamine function. In the rat, amphetamine-induced locomotion depends on the associated increase in limbic striatal dopamine release, and both of these indices are augmented in adult MAM-E17– exposed offspring (Flagstad et al 2004). Given the relevance of amphetamine-induced increases in striatal dopamine transmission to psychosis (Laruelle 2000; Weinberger and Lipska 1995), we examined whether the augmented response to amphetamine would emerge during or after puberty in the MAM-E17 model.

Methods and Materials

Drugs

Methylazoxymethanol acetate was obtained from Midwest Research Institute (Kansas City, Missouri, www.mriresearch.org); other drugs were obtained from RBI/Sigma (St. Louis, Missouri, www.sigma.com). Drugs were dissolved in isotonic saline.

Subjects

Timed-pregnant Fischer 344 dams were treated with MAM (22 mg/kg, intraperitoneal [IP]) or saline on E15 or E17. Within 4 days after birth, the litters were culled to 10 and then weaned and double-housed on postnatal day 28 (P28); one quarter of the litters was cross-fostered. Experiments were conducted on male animals at either P35 to P40 or 4 to 8 months of age, unless otherwise noted. At least four control and MAM-treated litters were included in each experiment. All procedures were approved by the University of Pittsburgh International Animal Care and Use Committee (IACUC) and adhered to the *Guide for the Care and Use of Laboratory Animals* (National Academy of Sciences 1996).

Neuroanatomy

Tissue Preparation and Microscopy—Adult rats were perfused with cold heparinized saline and then phosphate-buffered 4% paraformaldehyde. Brains were postfixed for 24 to 72 hours, cryoprotected in ascending sucrose solutions, and then cryosectioned in serial, 60-μm coronal sections. Every third section was mounted and stained with a neutral red: cresyl violet mixture. Brains were processed in yoked sets (control/MAM-E15/MAM-E17 or control/MAM-E17) to control fixation and tissue processing effects. Shrinkage in the coronal plane (76% ± 5%) was determined to be equal across control and MAM-treated groups prior to quantification of brain region size or neuron number. Sections were examined with a Zeiss Axioscope microscope (Carl Zeiss, Thornwood, New York) interfaced with a motorized stage (Ludl Electronic Products, Hawthorne, New York), digital video camera (DVC, Austin, Texas), and PC-based stereology system (MicroBrightfield, Inc., Williston, Vermont).

Thickness and Area Measurements—Multiple brain regions were assessed to determine the overall pattern and selectivity of neuroanatomical effects of maternal MAM exposure. Cross-sectional thickness or area measurements were taken from the prefrontal cortex (PFC) (an average of anterior cingulate and prelimbic regions), frontoparietal cortex (PAR), ventral perirhinal (PRH) (perirhinal and lateral dorsal entorhinal region ventral to the rhinal sulcus) and occipital (OCC) (area OcL2) cortices, as well as the hippocampus (HIPP). The borders of cortical regions could potentially have been affected by MAM exposure; thus, for each cortical region, we used a central starting location that on the basis of shape, cytoarchitechtonics, and position relative to subcortical structures (Paxinos and Watson 1986; Zilles and Wree 1995) was determined to be equivalent across control and MAM-exposed brains. Each region was then systematically sampled for up to 120 microns anterior and posterior to the starting point. Sampling regions excluded transitional zones between cortical regions, allowing greater homology across experimental groups. The anterior cingulate (Cg1, posterior dorsal Cg3) and prelimbic (Cg3) cortices were sampled between the level of the olfactory tubercle and rostral nucleus accumbens (Figure 1A). The frontoparietal cortex (Par1 in Zilles and Wree 1995) was sampled at the level of the anterior commissure. The perirhinal cortex ventral to the rhinal sulcus and the OcL2 subregion of the occipital cortex were sampled at the level of the medial geniculate nucleus (Figure 1C). Cortical thickness was defined as the length of the line perpendicular to the pial surface extended to the white matter (Figure 1A–C).

The more clearly definable borders of the hippocampus allowed the use of area as the size index (Figure 1B, C). The area at dorsal hippocampus at the level of the medial habenula and dorsal hippocampal commissure was calculated from the maximal dorsoventral and mediolateral segments (Figure 1B). The area of the caudal hippocampus was measured at the level of the substantia nigra pars compacta and medial geniculate body and was defined as the product of the maximal length of a segment along the long axis and the segment perpendicular to the long axis (Figure 1C).

In the thalamus, the area of the mediodorsal, paraventricular, intermediodorsal, and central medial thalamic nuclei combined was measured in sections in which the ventrolateral nucleus appeared (Paxinos and Watson 1986; Price 1995). The maximum area was calculated as the product of the length of the segments as shown in Figure 1B. The area of the medial geniculate nucleus and width of the central tegmentum were determined at the level of the substantia nigra pars compacta (Figure 1C). The dorsoventral thickness of the anterior cerebellar vermis was measured along the midline of this structure at levels containing the central gray area (Figure 1D).

The effect of gestational treatment (groups: control, MAM-E15, MAM-E17) on the size of each brain region was analyzed with a one-way analysis of variance (ANOVA). Planned, pairwise comparisons were made using Student *t* tests. Correlations of across brain regions or between the size of a brain region and a specific behavior were tested using Pearson one-tailed analyses.

Stereologic Determination of Neuron Number and Density in Cerebral Cortical Regions—The histology and microscopy methods used were as described above. To estimate total cortical neuron number, three anterior-posterior zones of the neocortex were sampled (nomenclature according to Paxinos and Watson 1986): 1) the prefrontal/cingulate/retrosplenial zone, consisting of the prelimbic, infralimbic, cingulate, retrosplenial, and medial occipital regions; 2) the parietal/lateral occipital zone, consisting of the parietal cortex (S1) continuing laterally to the dorsomedial border of parietal region S2 and posteriorally through the occipitotemporal region OcL2 to the dorsal border of auditory association cortex; and 3) the insular/perirhinal zone, including all of the insular cortex and perirhinal cortex. Although together they comprise the majority of the neocortex, these cortical zones differ in their developmental time courses (Bayer and Altman 1995) and, as such, could be differentially affected by MAM-E17 treatment. The total number of neuronal profiles in each zone was determined by applying an optical fractionator method modified from that of West et al (1991). The grand sum across all three regions was used as a representative “total” cortical neuron number.

In addition, neuronal density (cell number/sample volume) was calculated in the three zones, as well as in the regions used to sample cortical thickness, including the PFC (prelimbic and anterior cingulate combined), PAR, PRH, and OCC. As for the cortical thickness measurements, the transitional regions were avoided and a systematic sampling of sections determined to be unambiguously within the region of interest were used. Neuron number and volume for each sampling region were determined with a combination of the optical fractionator and Cavalieri estimation methods. Data were analyzed as a function of MAM treatment and brain region using two-way ANOVAs. Planned comparisons between treatment groups for each brain region were made with Student *t* tests.

Neurophysiology

The intracellular sharp electrode recording methods have been described in previous reports from our laboratory (West et al, submitted). Briefly, adult rats were anesthetized with chloral hydrate and mounted in the stereotaxic instrument; then a sharp glass microelectrode (60–80 MOhm impedance) filled with 2 mol/L potassium acetate was lowered into the medial PFC (at 2–4 mm anterior to Bregma, .5 mm from the midline) or ventral striatum (vSTR) (1.8 mm anterior, .9 mm from midline, 4–6 mm deep). After achieving a stable recording (membrane potential more negative than −55 mV, spike widths less than 1.7 milliseconds, evoked-spike heights greater than 60 mV) for at least 5 minutes, passive membrane properties and spontaneous shifts in membrane potentials in PFC and vSTRl

neurons were determined. Data were analyzed with nonparametric binomial and chi-square tests.

Behavioral Analyses

Motor Control in MAM-E17 and MAM-E15 Offspring—Adult control, MAM-E17, or MAM-E15 offspring were treated with saline or phencyclidine (PCP) (5.0 mg/kg, IP) and placed in a Plexiglas chamber (12” length × 10” width × 8” height) in a room illuminated with dim red light. Behavior was monitored by an observer blind to the condition of the animals and to the drug administered. Motor activity and ataxia were scored every 5 minutes using a modification of the scales developed by Sturgeon et al (1979) that capture both locomotor activity and stereotypy.

Prepulse Inhibition of Startle—Rats were placed in startle chambers (San Diego Instruments, Inc., San Diego, California) and habituated to a background noise level of 55 dB for 5 minutes, after which their startle threshold was determined with a repeated ascending, then randomized, series of 40-millisecond noise bursts ranging from 70 to 105 dB. After the startle threshold was determined, prepulse inhibition of startle (PPI) was quantified with a modification of established methods (Lipska et al 1995; Swerdlow et al 1999) using a 55 dB background (white noise), 100 dB startle tone (white noise burst), prepulses from 7 to 15 dB above background and 6 or 12 milliseconds duration, and intertrial intervals of 15 ± 6 seconds. Prepulses were presented on 75% of the startle trials. Startle threshold (dB) and maximal startle response (arbitrary force units) were compared across control and MAM-exposed rats with Student independent *t* tests. Prepulse inhibition of startle at each prepulse salience level was quantified as a percent change from average displacement on nonprepulse trials and analyzed with a mixed ANOVA with treatment group as the between-subjects factor and prepulse salience as the repeated measure.

Orofacial Dyskinesia—Rats were injected with saline or PCP (2.5 or 5.0 mg/kg, IP) and transferred to a novel clear Plexiglas chamber (12” length × 10” width × 8” height) located in a red-light illuminated room. Oral behaviors were quantified by direct observation (by an observer blind to gestational and drug conditions) and were defined as follows: tremor, rapid oscillation of facial muscles progressing from lower jaw through cheek to extraocular region; stereotypic mouthing of the tail, repetitive approaches to the tail with the mouth featuring horizontal and vertical motions of the jaw (follow-through biting rarely occurred). At every 5 minutes following drug administration, these behaviors were scored as absent (0), present/intermittent (1), or continuous (2). The effect(s) of gestational treatment and PCP were analyzed for each behavioral variable with an ANOVA including gestational treatment and PCP as factors. Main effects and interactions were analyzed using Student-Neuman-Keuls tests.

Reversal Learning—The Y-maze (HabiTest; Coulbourn Instruments, Allentown, Pennsylvania) consisted of a central chamber with guillotine doors opening into three 36-inch runways, each terminating in a food magazine. Adult female control rats and MAM-E17 rats were habituated to the Y-maze then trained in the conditional discrimination task. In this task, the rat was placed in an arm and the trial was initiated by the opening of the door to the central chamber. Three seconds later, the doors to the choice arms opened and each food magazine was illuminated with a constant or flashing (120 Hz) light (the spatial position of the two cues were randomized across trials). A head poke into the CS+ magazine resulted in the termination of the light and delivery of two 45-mg sweetened food pellets (BioServ, San Diego, California). A poke into the CS^{-} magazine resulted in termination of the light and a 15-second time-out. The next trial was initiated from the choice arm of the previous trial; sessions were 30 trials long. After the rat achieved 67% accuracy for 3

consecutive days, the reward contingency was reversed (i.e., the CS+ became the CS^- and visa versa). The number of trials to criterion for acquisition and reversal phases were compared between MAM-E17 rats and control rats with Student *t* tests.

Locomotor Response to Amphetamine at Prepubertal and Postpubertal Ages—Within litters, half of the pups were tested at P35–P40, the other half at 4 months. Before testing, rats were habituated to handling and to the testing room. On the test day, during their dark cycle, animals were placed in an activity monitor with two 17 × 17 grids of infrared beams with 1-inch spacing located 1.5 and 7.5 inches above the floor (Truscan, Coulbourn Instruments, Allentown, Pennsylvania). Ambulation (continuous movement across at least two squares) was recorded for 30 minutes prior to and 60 minutes after injection of saline or amphetamine (.5 mg/kg, IP). Postinjection ambulation was analyzed with a three-way (gestational condition × testing age × drug) ANOVA.

Results

Brain and Body Weight

Methylazoxymethanol acetate treatment did not affect gestational period or litter size. At 6 to 8 months, body weights of MAM-E17 offspring (400.0 ± 4.5 g) and saline-treated offspring (411 ± 5.2 g) were not significantly different. The weight of MAM-E17 brains (1.79 ± .01 g) was decreased by about 7.0% compared with matched control brains [1.92 ± .02 g; $t(32) = 5$, $p < .001$]. Although the body weights of MAM-E15 were not markedly decreased, their brains were significantly smaller compared with either control rats or MAM-E17 rats [1.39 ± .02, $t(24) = 11.2$, $p < .001$, relative to MAM-E17].

Histopathology in Limbic and Paralimbic Cortical and Thalamic Regions

Gross Morphology and Positions of Cortical and Subcortical Regions— Methylazoxymethanol acetate-E15 brains (Figure 2C; Figure 3C, F) showed a marked, nonselective reduction in the size of all cortical and subcortical regions. By contrast, in MAM-E17 brains (Figure 2B; Figure 3B, E), subcortical regions appeared normal; however, the cerebral cortex, especially the hippocampus, appeared to be slightly reduced in size, resulting in an anterior "shift" or constriction of the posterior border.

Methylazoxymethanol acetate treatment significantly affected the sizes of all brain regions [all F's ($df = 2, 28–36$) > 4.0, $p < .05$] except the cerebellar vermis (p > .2). Moreover, these effects depended on the embryonic timing of the exposure. Independent *t* tests (equal variances not assumed) revealed that MAM-E15 rats exhibited significant decreases in all brain regions, except the cerebellar vermis, when compared with either control or MAM-E17 brains [all t's (7–22) > 3.0, p's < .05) (Figure 4A–D). On the other hand, the MAM-E17 model showed a more selective and schizophrenia-relevant pattern of reductions in gray matter. Methylazoxymethanol acetate-E17 rats exhibited significant decreases in thickness of the PFC [$t(9.2) = 4.3$, $p < .05$], PRH [$t(14) = 3.0$, $p < .01$], OCC [$t(8) = 3.1$, $p < .05$], and HIPP [$t(9.5) = 2.7$, $p < .05$], with no difference in the PAR [$t(8) < 1.4$, $p > .1$] (Figure 4A, B). Subcortically, MAM-E17 rats showed a significant decrease in the area of the mediodorsal (MD) [$t(8) = 2.9$, $p < .05$], a trend toward a smaller medial geniculate body (MG) [$t(6) = .061$), with no differences in the sizes of the tegmentum (TEG) ($p > .3$) or cerebellum (CBL) (p's = .2) (Figure 4C, D).

Stereological analyses revealed that MAM-E17 and control offspring did not differ in the total number of neurons in the prefrontal/cingulate, insular/perirhinal, and parietal/lateral occipital cortical zones ["grand total" analysis: control, 5.75 (± .86) × 10^6; MAM-E17, 4.60 (± .69) × 10^6; $F(1,10) = .93$, $p > .3$]. However, a significant interaction between gestational

condition and cortical zone [$F(2,20) = 14.8$, $p < .05$] was found. When each cortical zone was analyzed separately, although total neuron number was not different between MAM-E17 and control offspring in each zone, there was a significant increase in density in the prefrontal/cingulate [$t(10) = 2.3$, $p = .05$] and insular/perirhinal [$t(10) = 1.97$, $p = .07$] zones, with no difference in neuronal density in the parietal/lateral occipital zone [$t(10) = 1.3$, $p > .2$].

In an additional set of brains, we determined whether MAM-E17 treatment produced an increase in neuronal density specifically in the medial prefrontal and occipital cortices but not in a lateral frontal region (frontoparietal cortex) (Selemon et al 1995, 2003). The perirhinal cortex was also examined. Figure 5A illustrates cell distribution and density in a section of the prelimbic cortex in age-matched control rats and MAM-E17 rats. As shown in Figure 5B, in MAM-E17 rats, neuronal density was increased in the PFC [$t(8) = 2.4$, $p < .05$], PRH [$t(8) = 2.9$, $p < .05$], and OCC [$t(6) = 2.8$, $p < .05$] but not in the PAR ($p > .2$). The thickness measurements of cortical regions of these brains, conducted as described above, were within the ranges reported above for control (CON) rats and MAM-E17 rats (data not shown).

A third set of brains (from different litters) was used to determine if the effects of MAM on neuronal density in the PFC, PRH, and PAR were robust, as well as to test the hypothesis that there was a significant difference in MAM-E17 treated brains on neuronal density in the PFC when compared with the PAR. In this analysis, a mixed ANOVA using gestational condition as a factor and brain region (PFC, PRH, and PAR) as the repeated measure revealed a significant interaction between gestational treatment and brain area [$F(2,20) = 7.3$, $p < .01$]. A similar ANOVA including only the PFC and PAR revealed a significantly different effect of MAM-E17 treatment on PFC relative to PAR. *T* tests replicated the results of the first cohort of brains with both PFC [$t(10) = -2.4$, one-tailed $p < .02$] and PRH [$t(10) = -2.0$, one-tailed $p < .05$] but not PAR [$t(10) = +1.3$, $p > .2$]. Thus, stereological analyses conducted on two independent sets of MAM brains showed increases in neuronal density in the PFC, PRH, and OCC, areas in which thickness was significantly decreased. On the other hand, neuronal density in the frontoparietal cortex was significantly less affected than in the PFC. This loss of intercellular matrix and reduction in cortical thickness occurred in the absence of a significant difference in total neuron number across large cerebral cortical zones.

Neurophysiological Properties of PFC and Ventral Striatal Neurons

Because of the more selective and schizophrenia-relevant pattern of histopathology in the MAM-E17 rats, neurophysiology experiments were conducted only in this model. In vivo sharp-electrode intracellular recordings of PFC and vSTR neurons revealed abnormalities in the membrane properties and sub-threshold transitions of the membrane potential. Analysis of the membrane properties of PFC neurons revealed that MAM-E17 PFC neurons showed a significantly more depolarized resting membrane potential [Table 1; $t(32) = -2.9$, $p < .01$]; however, the spike threshold was also more depolarized than in control rats [Table 1; $t(25) = -2.27$, $p < .05$]. Thus, the amplitude depolarization from the average resting state necessary to generate a spike (spike threshold Δ) was comparable between CON rats and MAM-E17 rats (Table 1; $p > .5$). Methylazoxymethanol acetate-E17 PFC neurons also showed significantly higher input resistances relative to CON rats [Table 1; $t(24) = -2.2$, $p < .05$].

Prefrontal cortex and vSTR neurons were classified as exhibiting a bistable membrane potential if the time amplitude histogram of the membrane potential sampled across 1 minute (.5 second bins) exhibited two distinct modes: a resting (down) state at about −74 mV or −80 mV in PFC and vSTR neurons, respectively, and a second distinct mode at least 8 mV more depolarized with respect to the resting state (Figure 6, inserts). Consistent with

previous reports, the depolarized or "up" states occurred at an average frequency of .8 Hz and exhibited durations of 200 to 800 milliseconds. Compared with the PFC and vSTR neuron population in CON rats (16/21, expected value of .76), the proportion of bistable neurons in MAM-E17 rats was significantly decreased [5/16; χ^2 (*df*, 1) = 21.0, $p < .01$]. Thus, MAM-E17 rats exhibited a lack of up and down states in vSTR and PFC neurons. Rather, these neurons rested at membrane potentials significantly more depolarized than the down state of CON neurons (Table 1) and intermediate of the average down and up states of the CON neurons. Furthermore, the spike threshold was more depolarized in the MAM-E17 rats (Table 1). In CON rats, only bistable neurons were spontaneously active, and in these neurons, spikes were generated only from the up state. In contrast, although the average spike threshold was more depolarized in MAM-E17 rats, spikes appeared to be generated from the relatively depolarized, monostable resting potential (Figure 6), suggesting a loss of state-dependent spike firing.

Behavioral Abnormalities Consistent with Temporal and Frontal Corticostriatal Circuit Dysfunction

Gross Motor Abnormalities—The analysis of ataxia showed a significant effect of gestational treatment [$F(2,28) = 7.7$, $p < .01$; Figure 7] and a near-significant interaction between gestational treatment and PCP treatment [$F(2,28) = 3.2$, $p = .057$]. While MAM-E17 did not differ from CON rats, MAM-E15 rats showed a greater level of ataxia [$t(8)$'s > 2, $p < .05$] and a more marked ataxic effect of PCP [$t(8)$'s > 2, $p < .05$] than both other groups. On the other hand, the motor activity/stereotypy induced by PCP was increased in MAM-E15 and MAM-E17 offspring (relative to control rats) to similar degrees [main effect of gestational treatment, $F(2,28) = 3.9$, $p < .05$; *t* tests for MAM E17 and E15 vs. CON, $t(11)$'s > 2, $p < .05$]. Thus, in the MAM-E15 but not MAM-E17 model, motor stimulation was accompanied by an abnormal level of ataxia. Thus, further behavioral testing focused on the MAM-E17 model.

Prepulse Inhibition of Startle in the MAM-E17 Model—The prepulse conditions produced 40% to 85% prepulse inhibition in control rats, and MAM-E17 rats showed a deficit in prepulse inhibition [Figure 8; main effect of gestational condition, $F(1,36) = 4.72$, $p < .05$]. The prepulse inhibition deficit was not due to a decrease in sensory processing, since the MAM-E17 rats showed a lower threshold for responding to startle stimuli [control rats, 88 ± 1.2 dB; MAM-E17, 80 ± 3.2 dB, $t(15) = 2.7$, $p < .05$] nor was it due to a change in motor function, since the maximal startle responses of MAM-E17 rats did not differ from control rats [arbitrary units, control rats: @100 dB, 25.7 ± 3.5, @120 dB, 43.0 ± 6.3; MAM-E17: @100 dB 25.1 ± 2.4, @120 dB 40.9 ± 3.6; *t*'s (44) < .2, *p*'s < .8]. In the same experiment, prepulse inhibition was measured in six MAM-E15 offspring. These animals showed a decrease in startle amplitude compared with matched control rats [@120 dB, 29 ± 6.8, $t(12) = 3.1$, $p < .05$]. There was no decrease in PPI; however, the low statistical power of the experiment prevents interpretation of this as a negative effect.

Prefrontal Cortical Circuit Function—Methylazoxymethanol acetate treated rats displayed a significantly higher frequency of spontaneous orofacial dyskinesias and stereotypies; moreover, these behaviors were significantly more sensitive to exacerbation by PCP (Figure 9A). The level of orofacial dyskinesias was correlated with size of the caudal hippocampus (Pearson correlation = −.43, $p < .02$) (total orofacial dyskinesia) and the anterior cingulate subregion of the PFC (Pearson correlation = −.39, $p < .05$) but not with any other brain region examined.

Methylazoxymethanol acetate-E17 rats also showed a significant deficit in reversal learning. The mixed ANOVA revealed a significant interaction between gestational condition and

learning phase (acquisition vs. reversal) [$F(1,15) > 4$, $p < .05$]. Relative to control rats, MAM-E17 rats did not show a deficit in learning the novel discrimination; indeed, these rats learned the discrimination significantly faster than control rats (Figure 9B, left; $p < .01$), indicating that forebrain circuits involved in basic discriminated approach learning were not affected. However, under reversal conditions, MAM-E17 rats required significantly more trials to reach criterion than control rats (Figure 9B, right; $p < .01$).

Postpubertal Increase in the Responsiveness to Amphetamine—The ANOVA showed a significant three-way interaction among gestational treatment, testing age, and dose [$F(1,40) = 4.6$, $p < .05$]. Planned two-way ANOVAs revealed that prior to puberty (P35), control and MAM-E17 rats showed comparable increases in ambulation following amphetamine compared with saline [$F(1,15) = .15$, $p > .1$]. However, as adults, MAM E17 rats showed significantly greater response to amphetamine [Figure 10; $F(1,25) = 6.7$, $p < .05$].

Discussion

MAM, Gestational Timing, and Epigenetic Factors in the Etiology of Schizophrenia

The present experiments are novel in showing that in addition to exhibiting key behavioral abnormalities, such as sensorimotor gating deficits and cognitive inflexibility, the MAM-E17 model exhibits a schizophrenialike pattern of neuro(histo)pathology. The earlier MAM exposure on E15 led to marked microcephaly and gross motor impairments, including ataxia and a blunted startle reflex. The present data resolve a recent controversy in the evaluation of MAM exposure as a model of schizophrenia. Recently, Jongen-Relo et al (2004) reported that MAM at E15 and earlier, despite producing marked dysmorphology of the cortex, did *not* produce deficits in prepulse inhibition and thus concluded that prenatal MAM treatment does not produce a model of schizophrenia. Our behavioral and anatomical data limit this conclusion to MAM-E15 and perhaps earlier exposures. However, the present data and previous studies (Flagstad et al 2004; Gourevitch et al 2004) show that MAM-E17 exposure leads to deficits in prepulse inhibition as well as other behavioral and neuroanatomical characteristics that are highly relevant to schizophrenia.

Similar to most methyl donors, MAM methylates DNA and other nucleic acids (Nagata and Matsumoto 1969). It is not known, however, whether nucleic acid methylation underlies MAM's preferential effects on neurons, especially cortical neurons (Cattabeni and Di Luca 1997; Chevassus-Au-Louis et al 1998; Haddad et al 1972; Singh 1980). The DNA methylation may regulate the expression of reelin and GAD_{67}, genes that are downregulated in the cortex in schizophrenia (Dong et al 2005; Tremolizzo et al 2002). Perhaps MAM-induced methylation downregulates the expression of genes that are critical for cortical neuron development and plasticity (Fiore et al 1999), including genes involved in cortical gamma-aminobutyric acid (GABA) transmission (Ben-Ari et al 2004; Dong et al 2005; Penschuck et al 2005). In the context of these possibilities, it is important that the methylation patterns produced by MAM-E17 exposure, and the genes most affected by these patterns, are characterized.

Pattern of Histopathology in the MAM-E17 Model: Insights into Potential Developmental Pathways to the Neuropathology of Schizophrenia

Methylazoxymethanol acetate-E17 rats exhibit a number of neuroanatomical alterations that are consistent with that observed in the schizophrenia patient (see Table 2). Moreover, similar to what has been reported in schizophrenia (Bilder et al 1995; Wible et al 1995), the severity of the apparent tissue loss in the temporal lobe correlates frontal lobe dysfunction (orofacial dyskinesia) in this model. The pattern of neuropathology includes the medial

dorsal thalamic-prefrontal cortical circuit and a hippocampal entorhinal-perirhinal medial frontal circuit. The thalamic pathology likely involves reduced neuron number (Moore HM, unpublished observations, 2006) and may be secondary to a failure of the prefrontal corticothalamic pathway to develop properly. Previous studies have shown that MAM-induced disruption of cortical development causes a subsequent loss of neurons in the thalamus (Ashwell 1987). With regard the apparent sparing of the lateral frontal cortex, both the PFC-MD thalamus circuit and the occipitotemporal prefrontal circuits largely bypass the dorsolateral frontoparietal cortex in the rat. On the other hand, the ventral visual stream is interconnected with the limbic temporal cortex, medial frontal cortex, amygdala and limbic thalamus (Burwell and Amaral 1998; Insausti et al 1997; McDonald and Mascagni 1996), and lateral frontal regions (e.g., Brodmann area 45/Broca's area). Given that the development of a region depends on the synaptic connections made by both the afferents and efferents, the temporal limbic cortex and the lateral frontoparietal cortex may be the most and least vulnerable, respectively, to the "compounding" developmental effect of MAM exposure on E17. Such a model would predict, however, that thalamic regions receiving inputs from the hippocampus and perirhinal cortex should be affected similarly to the MD.

Sensorimotor Gating, the Augmented Response to Amphetamine and Dysregulation of Limbic and Dopamine Afferents to the Striatum

Methylazoxymethanol acetate-GD17 rats showed alterations in sensorimotor gating, with the magnitude of the deficit being similar to that reported in schizophrenia patients (Braff et al 1992). This is consistent with the effects of neonatal lesions of the ventral hippocampus (Lipska et al 1995). Moreover, both the increased responsiveness to amphetamine and the PPI deficit in the MAM-E17 model are consistent with abnormal limbic corticostriatal or mesolimbic dopamine transmission in this model (Caine et al 2001; Swerdlow et al 1999). Indeed, the histopathology of the hippocampus (this study) and associated abnormal synaptic transmission in the hippocampal-striatal pathway in the MAM-E17 model may underlie the PPI deficit. The developmental specificity of the abnormal response to amphetamine, specifically that this phenotype emerges during or after puberty, provides additional construct validity to the model (Geyer et al 2001; Moore et al 1999; Weinberger and Lipska 1995).

Dysfunction of the Frontal Corticostriatal Circuits

Both spontaneous and learned behaviors suggest a frontal cortical dysfunction in the MAM-E17 rat that is relevant to schizophrenia. Disruption of the frontal cortex in both rats and humans increases the susceptibility to orofacial dyskinesias (Gunne et al 1982; Waddington et al 1995). The present results are consistent with findings that MAM-E15 exposed offspring show higher susceptibility for chronic haloperidol-induced orofacial dyskinesias (Johansson 1990). Given that the striatal retogions innervated by the frontal cortex (i.e., medial and ventral striatum) mediate oral dyskinesias (Cools et al 1995; Hamid et al 1998; Prinssen et al 1996), the more potent effect of PCP on oral movements in the MAM-E17 animals is consistent with a hypo-function of the glutamatergic frontal corticostriatal pathway (Tamminga 1998).

The selective deficit in reversal learning in MAM-E17 rats suggests that: 1) cortical circuits involved in sensory and motor processes and association learning are intact; 2) the faster learning may be indicative of a perseverative response, in which the rats fail to test the nonrewarded arm once the association in the rewarded arm has been experienced; and 3) the perseveration is further revealed when the contingencies are reversed. Their learning phenotype is also consistent with the MAM-E17 rats being more sensitive to the negative consequences associated with the original CS^{-}. Each of these abnormalities implicates

frontal cortical function. Acquisition of a novel discrimination is not sensitive to frontal lesions, whereas reversal learning is significantly impaired in frontal lobe-lesioned and schizophrenia patients (Elliott et al 1995), as well as in rats with lesions or inactivation of the ventromedial and lateral orbital cortex (Chudasama and Robbins 2003). Orbitofrontal lesions impair reversal learning by causing a perseveration of responding to the previous CS +. On the other hand, lesions of the prelimbic/infralimbic regions impair the learning of a new contingency during a reversal, even in the absence of perseverative responding to a previous CS+ (Chudasama and Robbins 2003). This may be related to the importance of the medial PFC in extinction of aversive associations, e.g., the absence of reward associated with the CS^{-}. Impaired extinction of the aversive association with the former CS^{-} would reduce the probability of approaching the stimulus and retard learning of the new, appetitive association during the reversal. While orbital cortex was not examined specifically in the anatomical experiments, it was included in the insular/perirhinal zone, which showed increased neuronal density in the MAM-E17 model. The prelimbic/infralimbic region showed reduced size, increased neuronal density, and impaired synaptic activity. Thus, as with schizophrenia (Elliott et al 1995; Seidman et al 1994; Szeszko et al 2000), it is likely that abnormalities in multiple prefrontal regions contribute to the cognitive inflexibility in the MAM-E17 model.

The neurophysiological properties of PFC neurons and their striatal targets in the MAM-E17 model may provide insight into the significance of the cortical pathology for PFC regulation of behavior. In the normal brain in vivo, the neurons of the cerebral cortex and striatum regularly shift to depolarized states from which action potentials are selectively generated (Cowan and Wilson 1994; O'Donnell and Grace 1995; West et al, submitted). These "up" states are dependent on convergent activity of excitatory synaptic inputs to the neuron (Steriade 2001; West et al, submitted). The "bistable" property of cortical and striatal spiny neurons has been proposed to underlie the ability of these neurons to function as coincidence detectors (Konig et al 1996) and, as such, may subserve processes such as response selection. Indeed, the firing of the MAM-E17 neurons from the monostable state showed cortical and striatal "output" is no longer constrained by the convergence of cortical (and thalamic) signals to these neurons. The modulation of response selection by internal drives or environmental contingencies involves cortical, amygdalar, and dopaminergic inputs to the PFC and striatum (Jentsch et al 2000; Seamans et al 1998). Pathology in these circuits the loss of bistable membrane states in PFC and striatum neurons would reduce the probability that the PFC (e.g., representing a new response-outcome contingency) could "direct" output of the striatum (Moore et al 1999).

Summary and Conclusions

Methylazoxymethanol acetate-E17 exposure leads to the pattern of histopathology observed in schizophrenia. The model also shows homology at the level of behavioral evidence for dysfunction of the frontal cortex and limbic and dopaminergic inputs to striatum. The relevance to schizophrenia is further underscored by the evidence for a hyperresponsive mesostriatal dopamine system that develops during or after puberty. The neurophysiological abnormalities in the PFC and ventral striatum may represent mechanisms linking the subtle histopathology of schizophrenia with the psychopathology. Given these characteristics, this model may be useful in discovering drugs that would not be identified with traditional screens for antipsychotics, e.g., treatments aimed at normalizing frontal or temporal cortical function in schizophrenia. As a developmental model, it can also be used to identify genes that, via a disruption of the developmental regulation of their expression, contribute to the abnormal functional development of cortical circuits. Finally, perhaps the most innovative use of such a model may be to identify early behavioral and physiological abnormalities that may serve as biomarkers for preventative treatments.

Acknowledgments

This work was supported by National Alliance for Research on Schizophrenia and Affective Disorders Young Investigator (to HM) and Distinguished Investigator (to AAG) Awards; a Stanley Foundation Award (to HM, AAG); and United States Public Health Service (USPHS) MH 45156, MH 57440 (to AAG), and MH 52885 (to MAG). MAG holds an equity interest in San Diego Instruments, Inc.

References

Ananth H, Popescu I, Critchley HD, Good CD, Frackowiak RS, Dolan RJ. Cortical and subcortical gray matter abnormalities in schizophrenia determined through structural magnetic resonance imaging with optimized volumetric voxel-based morphometry. Am J Psychiatry. 2002; 159:1497–505. [PubMed: 12202269]

Andreasen NC, Carpenter WT Jr. Diagnosis and classification of schizophrenia. Schizophr Bull. 1993; 19:199–214. [PubMed: 8322032]

Andreasen NC, O'Leary DS, Flaum M, Nopoulos P, Watkins GS, Ponto LL Boles, et al. Hypofrontality in schizophrenia: Distributed dysfunctional circuits in neuroleptic-naive patients. Lancet. 1997; 349:1730–1734. [PubMed: 9193383]

Archer T, Fredriksson A, Sundstrom E, Luthman J, Lewander T, Soderbert U, et al. Prenatal methylazoxymethanol treatment potentiates d-amphetamine- and methylphenidate-induced motor activity in male and female rats. Pharmacol Toxicol. 1988; 63:233–239. [PubMed: 3194344]

Ashwell K. Direct and indirect effects on the lateral geniculate nucleus neurons of prenatal exposure to methylazoxymethanol acetate. Brain Res. 1987; 432:199–214. [PubMed: 3676837]

Bayer, SA.; Altman, J. Neurogenesis and neuronal migration. In: Paxinos, G., editor. The Rat Nervous System. 2nd ed. Academic Press; San Diego: 1995. p. 1041-1078.

Ben-Ari Y, Khalilov I, Represa A, Gozlan H. Interneurons set the tune of developing networks. Trends Neurosci. 2004; 27:422–427. [PubMed: 15219742]

Bertolino A, Roffman JL, Lipska BK, van Gelderen P, Olson A, Weinberger DR. Reduced N-acetylaspartate in prefrontal cortex of adult rats with neonatal hippocampal damage. Cereb Cortex. 2002; 12:983–990. [PubMed: 12183397]

Bilder RM, Bogerts B, Ashtari M, Wu H, Alvir JM, Jody D, et al. Anterior hippocampal volume reductions predict frontal lobe dysfunction in first episode schizophrenia. Schizophr Res. 1995; 17:47–58. [PubMed: 8541249]

Braff DL, Grillon C, Geyer MA. Gating and habituation of the startle reflex in schizophrenic patients. Arch Gen Psychiatry. 1992; 49:206–215. [PubMed: 1567275]

Burwell RD, Amaral DG. Cortical afferents of the perirhinal, postrhinal, and entorhinal cortices of the rat. J Comp Neurol. 1998; 398:179–205. [PubMed: 9700566]

Caine SB, Humby T, Robbins TW, Everitt BJ. Behavioral effects of psychomotor stimulants in rats with dorsal or ventral subiculum lesions: Locomotion, cocaine self-administration, and prepulse inhibition of startle. Behav Neurosci. 2001; 115:880–894. [PubMed: 11508727]

Cattabeni F, Di Luca M. Developmental models of brain dysfunctions induced by targeted cellular ablations with methylazoxymethanol. Physiol Rev. 1997; 77:199–215. [PubMed: 9016302]

Chevassus-Au-Louis N, Congar P, Represa A, Ben-Ari Y, Gaiarsa JL. Neuronal migration disorders: Heterotopic neocortical neurons in CA1 provide a bridge between the hippocampus and the neocortex. Proc Natl Acad Sci U S A. 1998; 95:10263–10268. [PubMed: 9707635]

Chudasama Y, Robbins TW. Dissociable contributions of the orbitofrontal and infralimbic cortex to pavlovian autoshaping and discrimination reversal learning: Further evidence for the functional heterogeneity of the rodent frontal cortex. J Neurosci. 2003; 23:8771–8780. [PubMed: 14507977]

Clark L, Cools R, Robbins TW. The neuropsychology of ventral prefrontal cortex: Decision-making and reversal learning. Brain Cogn. 2004; 55:41–53. [PubMed: 15134842]

Cools AR, Miwa Y, Koshikawa N. Role of dopamine D1 and D2 receptors in the nucleus accumbens in jaw movements of rats: A critical role of the shell. Eur J Pharmacol. 1995; 286:41–47. [PubMed: 8566150]

Cowan RL, Wilson CJ. Spontaneous firing patterns and axonal projections of single corticostriatal neurons in the rat medial agranular cortex. J Neurophysiol. 1994; 71:17–32. [PubMed: 8158226]

Coyle JT, Singer H, Beaulieu M, Johnston MV. Development of central neurotransmitter-specified neuronal systems: Implications for pediatric neuro-psychiatric disorders. Acta Neurol Scand. 1984; 70:1–11. [PubMed: 6147947]

Dambska M, Haddad R, Kozlowski PB, Lee MH, Shek J. Telencephalic cytoarchitectonics in the brains of rats with graded degrees of micrencephaly. Acta Neuropathol (Berl). 1982; 58:203–209. [PubMed: 7158299]

Dong E, Agis-Balboa RC, Simonini MV, Grayson DR, Costa E, Guidotti A. Reelin and glutamic acid decarboxylase67 promoter remodeling in an epigenetic methionine-induced mouse model of schizophrenia. Proc Natl Acad Sci U S A. 2005; 102:12578–12583. [PubMed: 16113080]

Elliott R, McKenna PJ, Robbins TW, Sahakian BJ. Neuropsychological evidence for frontostriatal dysfunction in schizophrenia. Psychol Med. 1995; 25:619–630. [PubMed: 7480441]

Eriksdotter-Nilsson M, Jonsson G, Dahl D, Bjorklund H. Astroglial development in microencephalic rat brain after fetal methylazoxymethanol treatment. Int J DevNeurosci. 1986; 4:353–362.

Fiore M, Talamini L, Angelucci F, Koch T, Aloe L, Korf J. Prenatal methylazoxymethanol acetate alters behavior and brain NGF levels in young rats: A possible correlation with the development of schizophrenia-like deficits. Neuropharmacology. 1999; 38:857–869. [PubMed: 10465689]

Flagstad P, Mork A, Glenthoj BY, van Beek J, Michael-Titus A, Didriksen M. Disruption of neurogenesis at gestational day 17 in the rat causes behavioral changes relevant to positive and negative schizophrenia symptoms and alters amphetamine-induced dopamine release in the nucleus accumbens. Neuropsychopharmacology. 2004; 29:2052–2064. [PubMed: 15199377]

Geyer MA, Krebs-Thomson K, Braff DL, Swerdlow NR. Pharmacological studies of prepulse inhibition models of sensorimotor gating deficits in schizophrenia: A decade in review. Psychopharmacologia. 2001; 156:117–154.

Gourevitch R, Rocher C, Le Pen G, Krebs MO, Jay TM. Working memory deficits in adult rats after prenatal disruption of neurogenesis. Behav Pharmacol. 2004; 15:287–292. [PubMed: 15252279]

Grace AA. Cortical regulation of subcortical dopamine systems and its possible relevance to schizophrenia. J Neural Transm Gen Sect. 1993; 91:111–134. [PubMed: 8099795]

Grace, AA.; Moore, H. Regulation of information flow in the nucleus accumbens: A model for the pathophysiology of schizophrenia. In: Lenzenweger, MF.; Dworkin, RH., editors. Origins and Development of Schizophrenia: Advances in Experimental Psychopathology. American Psychological Association Press; Washington, DC: 1998. p. 123-160.

Gunne LM, Growdon J, Glaeser B. Oral dyskinesia in rats following brain lesions and neuroleptic drug administration. Psychopharmacology (Berl). 1982; 77:134–139. [PubMed: 6126902]

Haddad RK, Rabe A, Dumas R. Comparison of effects of methylazoxymethanol acetate on brain development in different species. Fed Proc. 1972; 31:1520–1523. [PubMed: 4626772]

Hamid EH, Hyde TM, Baca SM, Egan MF. Failure to down regulate NMDA receptors in the striatum and nucleus accumbens associated with neuroleptic-induced dyskinesia. Brain Res. 1998; 796:291–295. [PubMed: 9689480]

Hanlon FM, Sutherland RJ. Changes in adult brain and behavior caused by neonatal limbic damage: Implications for the etiology of schizophrenia. Behav Brain Res. 2000; 107:71–83. [PubMed: 10628731]

Harrison PJ. The neuropathology of schizophrenia. A critical review of the data and their interpretation. Brain. 1999; 122:593–624. [PubMed: 10219775]

Harrison PJ. The hippocampus in schizophrenia: A review of the neuropathological evidence and its pathophysiological implications. Psychopharmacology (Berl). 2004; 174:151–162. [PubMed: 15205886]

Insausti R, Herrero MT, Witter MP. Entorhinal cortex of the rat: Cytoarchitectonic subdivisions and the origin and distribution of cortical efferents. Hippocampus. 1997; 7:146–183. [PubMed: 9136047]

Jentsch, JD.; Olausson, P.; Moore, H. Animal models of psychosis. In: Soares, JC.; Gershon, S., editors. Handbook of Medical Psychiatry. 2nd ed. Mercel Dekker, Inc.; New York: 2003. p. 317-333.

Jentsch JD, Roth RH, Taylor JR. Role for dopamine in the behavioral functions of the prefrontal corticostriatal system: Implications for mental disorders and psychotropic drug action. Prog Brain Res. 2000; 126:433–453. [PubMed: 11105661]

Johansson P. Methylazoxymethanol (MAM)-induced brain lesion and oral dyskinesia in rats. Psychopharmacology (Berl). 1990; 100:72–76. [PubMed: 2296629]

Jongen-Relo AL, Leng A, Luber M, Pothuizen HH, Weber L, Feldon J. The prenatal methylazoxymethanol acetate treatment: A neurodevelopmental animal model for schizophrenia? Behav Brain Res. 2004; 149:159–181. [PubMed: 15129780]

Kabat K, Buterbaugh GG, Eccles CU. Methylazoxymethanol as a developmental model of neurotoxicity. Neurobehav Toxicol Teratol. 1985; 7:519–525. [PubMed: 4080069]

Kim J, Ragozzino ME. The involvement of the orbitofrontal cortex in learning under changing task contingencies. Neurobiol Learn Mem. 2005; 83:125–133. [PubMed: 15721796]

Konig P, Engel AK, Singer W. Integrator or coincidence detector? The role of the cortical neuron revisited. Trends Neurosci. 1996; 19:130–137. [PubMed: 8658595]

Laruelle M. The role of endogenous sensitization in the pathophysiology of schizophrenia: Implications from recent brain imaging studies. Brain Res Brain ResRev. 2000; 31:371–384.

Lewis DA, Levitt P. Schizophrenia as a disorder of neurodevelopment. Annu Rev Neurosci. 2002; 25:409–432. [PubMed: 12052915]

Lipska BK, Swerdlow NR, Geyer MA, Jaskiw GE, Braff DL, Weinberger DR. Neonatal excitotoxic hippocampal damage in rats causes postpubertal changes in prepulse inhibition of startle and its disruption by apomorphine. Psychopharmacology (Berl). 1995; 122:35–43. [PubMed: 8711062]

Lipska BK, Weinberger DR. To model a psychiatric disorder in animals: Schizophrenia as a reality test. Neuropsychopharmacology. 2000; 23:223–239. [PubMed: 10942847]

Marenco S, Weinberger DR. The neurodevelopmental hypothesis of schizophrenia: Following a trail of evidence from cradle to grave. Dev Psychopathol. 2000; 12:501–527. [PubMed: 11014750]

McDonald AJ, Mascagni F. Cortico-cortical and cortico-amygdaloid projections of the rat occipital cortex: A Phaseolus vulgaris leucoagglutinin study. Neuroscience. 1996; 71:37–54. [PubMed: 8834391]

Mohammed AK, Jonsson G, Sundstrom E, Minor BG, Soderberg U, Archer T. Selective attention and place navigation in rats treated prenatally with methylazoxymethanol. Brain Res. 1986; 395:145–155. [PubMed: 3640654]

Moore H, Ghajarnia M, Geyer M, Jentsch JD, Grace AA. Selective disruption of prefrontal and limbic corticostriatal circuits by prenatal exposure to the DNA methylating agent methylazoxymethanol acetate: Anatomical, neurophysiological and behavioral studies. Schizophr Res. 2001; 49(suppl): 48.

Moore H, West AR, Grace AA. The regulation of forebrain dopamine transmission: Relevance to the pathophysiology and psychopathology of schizophrenia. Biol Psychiatry. 1999; 46:40–55. [PubMed: 10394473]

Moser MB, Moser EI. Functional differentiation in the hippocampus. Hippocampus. 1998; 8:608–619. [PubMed: 9882018]

Nagata Y, Matsumoto H. Studies on methylazoxymethanol: Methylation of nucleic acids in the fetal rat brain. Proc Soc Exp Biol Med. 1969; 132:383–385. [PubMed: 5344864]

National Academy of Sciences. Guide for the Care and Use of Laboratory Animals. National Research Council, Institute for Laboratory Animal Research, National Academy Press; Washington, DC: 1996.

O'Donnell P, Grace AA. Synaptic interactions among excitatory afferents to nucleus accumbens neurons: Hippocampal gating of prefrontal cortical input. J Neurosci. 1995; 15:3622–3639. [PubMed: 7751934]

O'Donnell P, Lewis BL, Weinberger DR, Lipska BK. Neonatal hippocampal damage alters electrophysiological properties of prefrontal cortical neurons in adult rats. Cereb Cortex. 2002; 12:975–982. [PubMed: 12183396]

Paxinos, G.; Watson, C. The Rat Brain in Stereotaxic Coordinates. Academic Press, Inc; San Diego: 1986.

Penschuck S, Flagstad P, Didriksen M, Leist M, Michael-Titus AT. Decrease in parvalbumin-expressing neurons in the hippocampus and increased phencyclidine-induced locomotor activity in the rat methylazoxymethanol (MAM) model of schizophrenia. Eur J Neuroscience. 2006; 23:279–284.

Price, JL. Thalamus. In: Paxinos, G., editor. The Rat Nervous System. Academic Press; San Diego: 1995. p. 629-647.

Prinssen EP, Heeren DJ, Cools AR. d-Sulpiride inhibits oral behaviour elicited from the nucleus accumbens of freely moving rats. Brain Res Bull. 1996; 39:101–107. [PubMed: 8846111]

Remijnse PL, Nielen MM, Uylings HB, Veltman DJ. Neural correlates of a reversal learning task with an affectively neutral baseline: An event-related fMRI study. Neuroimage. 2005; 26:609–618. [PubMed: 15907318]

Robbins TW. Dissociating executive functions of the prefrontal cortex. Philos Trans R Soc Lond B Biol Sci. 1996; 351:1463–1471. [PubMed: 8941958]

Seamans JK, Floresco SB, Phillips AG. D1 receptor modulation of hippocampal-prefrontal cortical circuits integrating spatial memory with executive functions in the rat. J Neurosci. 1998; 18:1613–1621. [PubMed: 9454866]

Seidman LJ, Pantelis C, Keshavan MS, Faraone SV, Goldstein JM, Horton NJ, et al. A review and new report of medial temporal lobe dysfunction as a vulnerability indicator for schizophrenia: A magnetic resonance imaging morphometric family study of the parahippocampal gyrus [see comment]. Schizophr Bull. 2003; 29:803–830. [PubMed: 14989416]

Seidman LJ, Yurgelun-Todd D, Kremen WS, Woods BT, Goldstein JM, Faraone SV, et al. Relationship of prefrontal and temporal lobe MRI measures to neuropsychological performance in chronic schizophrenia. Biol Psychiatry. 1994; 35:235–246. [PubMed: 8186328]

Selemon LD, Mrzljak J, Kleinman JE, Herman MM, Goldman-Rakic PS. Regional specificity in the neuropathologic substrates of schizophrenia: A morphometric analysis of Broca's area 44 and area 9. Arch Gen Psychiatry. 2003; 60:69–77. [PubMed: 12511174]

Selemon LD, Rajkowska G, Goldman-Rakic PS. Abnormally high neuronal density in the schizophrenic cortex. A morphometric analysis of prefrontal area 9 and occipital area 17. Arch Gen Psychiatry. 1995; 52:805–820. [PubMed: 7575100]

Shenton ME, Dickey CC, Frumin M, McCarley RW. A review of MRI findings in schizophrenia. Schizophr Res. 2001; 49:1–52. [PubMed: 11343862]

Singh SC. Deformed dendrites and reduced spine numbers on ectopic neurones in the hippocampus of rats exposed to methylazoxymethanolacetate. A Golgi-Cox study. Acta Neuropathol (Berl). 1980; 49:193–198.

Steriade M. Impact of network activities on neuronal properties in corticothalamic systems. J Neurophysiol. 2001; 86:1–39. [PubMed: 11431485]

Sturgeon RD, Fessler RG, Meltzer HY. Behavioral rating scales for assessing phencyclidine-induced locomotor activity, stereotyped behavior and ataxia in rats. Eur J Pharmacol. 1979; 59:169–179. [PubMed: 575093]

Swerdlow NR, Braff DL, Geyer MA. Cross-species studies of sensorimotor gating of the startle reflex. Ann N Y Acad Sci. 1999; 877:202–216. [PubMed: 10415651]

Szeszko PR, Bilder RM, Lencz T, Ashtari M, Goldman RS, Reiter G, et al. Reduced anterior cingulate gyrus volume correlates with executive dysfunction in men with first-episode schizophrenia. Schizophr Res. 2000; 43:97–108. [PubMed: 10858628]

Talamini LM, Ellenbroek B, Koch T, Korf J. Impaired sensory gating and attention in rats with developmental abnormalities of the mesocortex. Implications for schizophrenia. Ann N Y Acad Sci. 2000; 911:486–494. [PubMed: 10911899]

Tamminga CA. Schizophrenia and glutamatergic transmission. Crit Rev Neurobiol. 1998; 12:21–36. [PubMed: 9444480]

Thune JJ, Pakkenberg B. Stereological studies of the schizophrenic brain. Brain Res Brain Res Rev. 2000; 31:200–204. [PubMed: 10719149]

Tremolizzo L, Carboni G, Ruzicka WB, Mitchell CP, Sugaya L, Tueting P, et al. An epigenetic mouse model for molecular and behavioral neuropathologies related to schizophrenia vulnerability. Proc Natl Acad Sci U S A. 2002; 99:17095–17100. [PubMed: 12481028]

Tsuang MT, Stone WS, Faraone SV. Toward reformulating the diagnosis of schizophrenia [see comment]. Am J Psychiatry. 2000; 157:1041–1050. [PubMed: 10873908]

Waddington JL, Lane A, Larkin C, O'Callaghan E. The neurodevelopmental basis of schizophrenia: Clinical clues from cerebro-craniofacial dysmorphogenesis, and the roots of a lifetime trajectory of disease. Biol Psychiatry. 1999; 46:31–39. [PubMed: 10394472]

Waddington JL, O'Callaghan E, Buckley P, Madigan C, Redmond O, Stack JP, et al. Tardive dyskinesia in schizophrenia. Relationship to minor physical anomalies, frontal lobe dysfunction and cerebral structure on magnetic resonance imaging. Br J Psychiatry. 1995; 167:41–44.

Watanabe M, Shimizu K, Kodama Y, Takishima K, Mamiya G, Ichinowatari N. Potentiating effects of methamphetamine on the hyperactivity of microencephalic rats treated prenatally with methylazoxymethanol: Possible implication of hyperdopaminergia. Brain Res. 1995; 670:173–180. [PubMed: 7719720]

Weinberger DR, Lipska BK. Cortical maldevelopment, anti-psychotic drugs, and schizophrenia: A search for common ground. Schizophr Res. 1995; 16:87–110. [PubMed: 7577773]

West AR, Moore H, Grace AA. Direct examination of local regulation of membrane activity in striatal and prefrontal cortical neurons *in vivo* using simultaneous intracellular recording and microdialysis. J Pharmacology Exper Therapeutics. 2001:867–877.

West MJ, Slomianka L, Gundersen HJ. Unbiased stereological estimation of the total number of neurons in thesubdivisions of the rat hippocampus using the optical fractionator. Anat Rec. 1991; 231:482–497. [PubMed: 1793176]

Wible CG, Shenton ME, Hokama H, Kikinis R, Jolesz FA, Metcalf D, et al. Prefrontal cortex and schizophrenia. A quantitative magnetic resonance imaging study. Arch Gen Psychiatry. 1995; 52:279–288.

Wright IC, Rabe-Hesketh S, Woodruff PW, David AS, Murray RM, Bullmore ET. Meta-analysis of regional brain volumes in schizophrenia. Am J Psychiatry. 2000; 157:16–25. [PubMed: 10618008]

Zilles, K.; Wree, A. Cortex: Areal and laminar structure. In: Paxinos, G., editor. The Rat Nervous System. Academic Press; San Diego: 1995. p. 649-688.

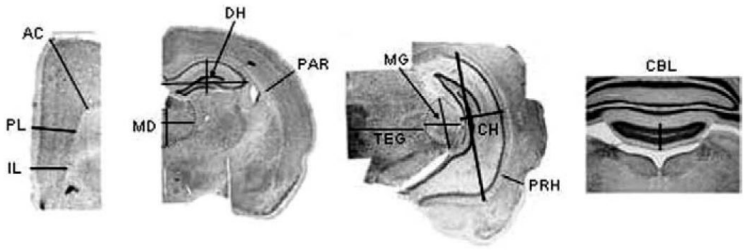

Figure 1.

Coronal sections of a control brain showing how cortical thicknesses and subcortical regional areas were measured. Size measurements were averaged from a set of five to seven coronal sections centered at the position shown. **(A)** Prefrontal cortex at the level of the rostral nucleus accumbens, where thicknesses of the anterior cingulate, prelimbic, and infralimbic cortices were measured. **(B)** The level of the rostral hippocampus and habenula where the areas of combined mediodorsal and anterior midline thalamic nuclei and the dorsal hippocampus were measured. The parietal cortex was measured more anteriorly, at the level of the anterior commissure, but at the dorsolateral position shown. **(C)** The level at which the tegmentum, medial geniculate body, caudal hippocampus, and perirhinal cortex were measured. **(D)** The level at which the thickness of the anterior vermis of the cerebellum was measured. AC, anterior cingulate; PL, prelimbic; IL, infralimbic; MD, mediodorsal and anterior midline thalamic nuclei; DH, dorsal hippocampus; PAR, parietal cortex; TEG, tegmentum; MG, medial geniculate body; CH, caudal hippocampus; PRH, perirhinal cortex; CBL, cerebellum.

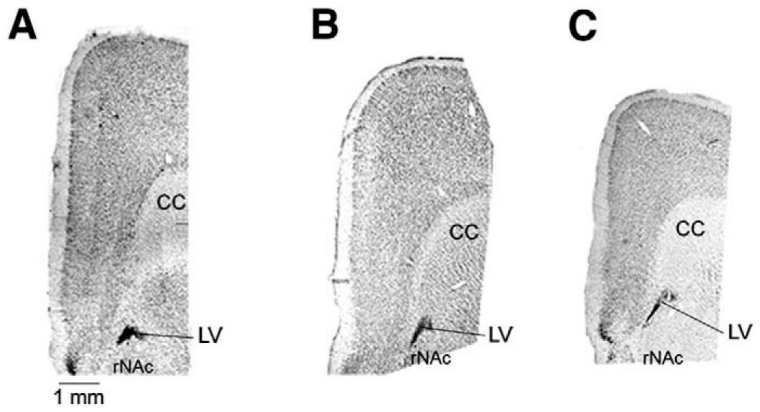

Figure 2.

Coronal sections of the prefrontal cortex at the level of the rostral nucleus accumbens in adult offspring of dams that were injected with **(A)** saline on E17 or E15, **(B)** MAM (22 mg/kg) on E17, or **(C)** MAM on E15. rNAc, rostral nucleus accumbens; MAM, methylazoxymethanol acetate; CC, corpus callosum; LV, lateral ventricle, anterior horn.

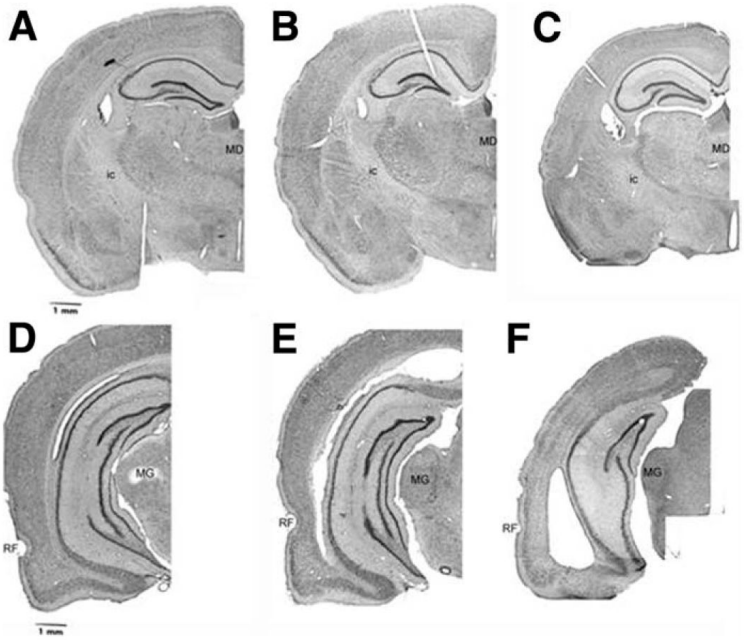

Figure 3.

Coronal sections at the level of the dorsal/rostral hippocampus and medial dorsal thalamus **(A–C)** and the caudal hippocampus and medial geniculate nucleus **(D–F)** in control **(A, D)**, MAM-E17 **(B, E)**, and MAM-E15 **(C, F)** rats. ic, internal capsule; MD, medial dorsal nucleus of the thalamus; RF, rhinal fissure; MG, medial geniculate body; MAM, methylazoxymethanol acetate.

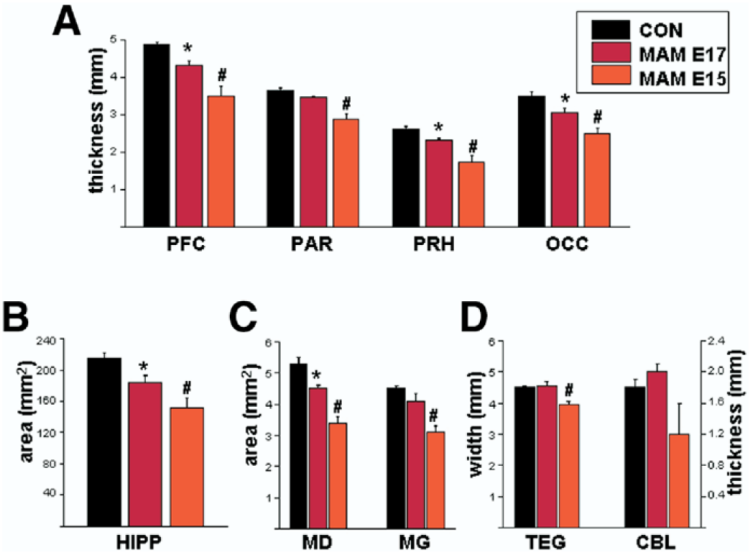

Figure 4.

Cerebral cortical thickness or area of cortical and subcortical regions of the adult offspring of CON (black bars), MAM-E17 (dark red bars), or MAM-E15 (orange bars) offspring. Locations of measurements are shown in Figure 1. **(A)** Thickness measurements of the prefrontal (the average of anterior cingulate and prelimbic; see Figure 1), frontoparietal, ventral perirhinal, and occipital area Oc2L. **(B)** The summed area of the rostral and caudal hippocampus. **(C)** Area of the medial dorsal and medial geniculate thalamic nuclei. **(D)** The width of the central tegmentum at the coronal level of the medial geniculate and the dorsal/ventral thickness of the anterior vermis of the cerebellum. Locations of measurements are shown in Figure 1. ANOVAs revealed a significant effect of MAM treatment for all areas (see text). $^{*}p < .05$ compared with control rats, $^{\#}p < .05$ compared with control rats or MAM-E17 rats, Student *t* test. CON, control; MAM, methylazoxymethanol acetate; PFC, prefrontal cortex; PAR, frontoparietal cortex; PRH, perirhinal cortex; OCC, occipital; HIPP, hippocampus; MD, medial dorsal nucleus of the thalamus; MG, medial geniculate body; TEG, tegmentum; CBL, cerebellum; ANOVA, analysis of variance.

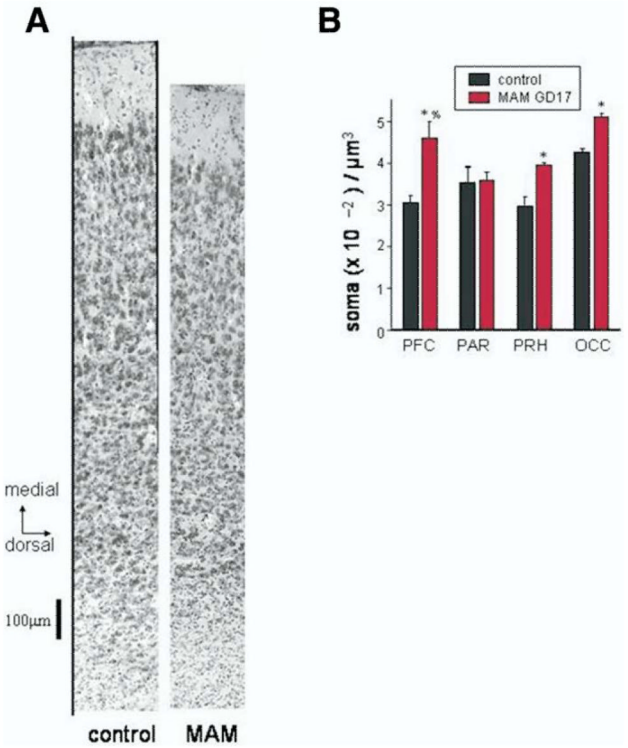

Figure 5.

Neuronal density in the prefrontal and other cortical region in control and MAM-E17 rats. **(A)** Photomicrograph of a cross-section of the prelimbic cortex of a control rat and a MAM-E17 rat. The orientation is rotated 90° with the corpus callosum at the bottom and the pial surface at the top. **(B)** Neuronal density was significantly increased in prefrontal cortex (PFC = AC + PL + IL), PRH, and OCC, but not in PAR in MAM-E17 rats. *MAM-E17 versus control rats, $t(10) > 3.8$, $p < .05$; %greater relative increase in density compared with PAR, $p < .05$. MAM, methylazoxymethanol acetate; PFC, prefrontal cortex; AC, anterior cingulate; PL, prelimbic; IL, infralimbic; PRH, perirhinal cortex; OCC, occipital; PAR, frontoparietal cortex.

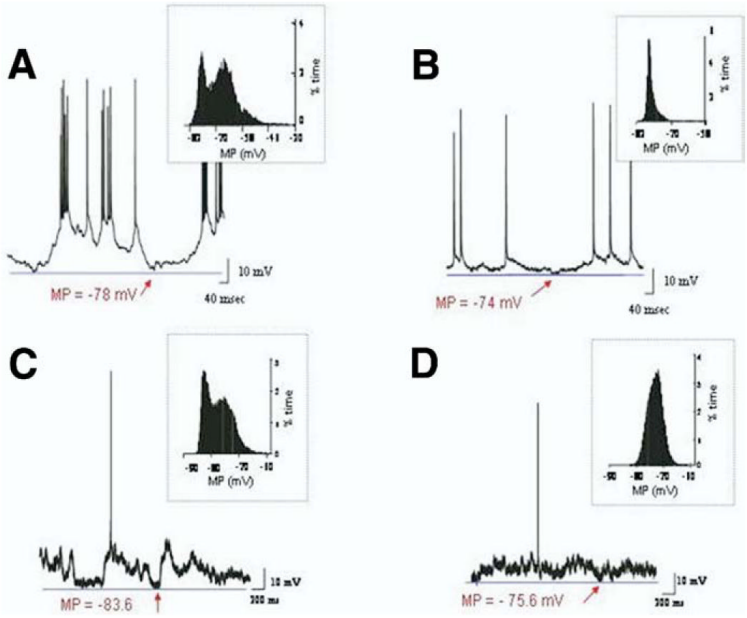

Figure 6.

Examples of spontaneous membrane activity in PFC **(A, B)** and vSTR **(C, D)** projection neurons in anesthetized control **(A, C)** and MAM-E17 **(B, D)** rats. Control neurons in the PFC **(A)** and vSTR **(C)** displayed spontaneous shifts from a hyperpolarized resting membrane potential (horizontal blue line) without spike firing to a depolarized state characterized by increased synaptic activity and spike firing. In MAM-E17 rats, PFC **(B)** and vSTR **(D)** neurons exhibited a monostable potential with spikes generated from this state. Panel insets. The bistable membrane potential is characterized by a bimodal distribution of the proportion of time spent at a given membrane potential within a range from the most hyperpolarized membrane potential to the spike threshold. The proportion of bistable PFC and vSTR neurons in MAM-E17 rats was significantly less than in control rats (chi-square analysis, $p < .01$). PFC, prefrontal cortex; vSTR, ventral striatum; MAM, methylazoxymethanol acetate.

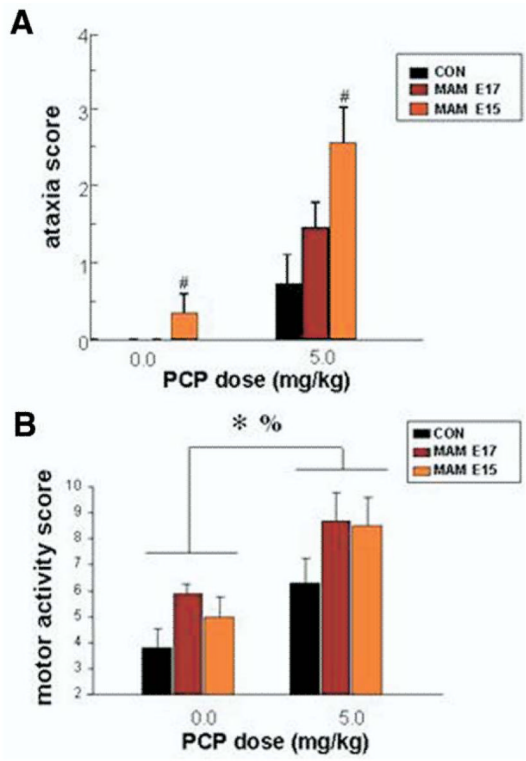

Figure 7.

(A) Ataxia in adult control or MAM-E17 offspring. Rats were placed in a clean standard rat cage in a dimly lit room following injection of saline or PCP (5.0 mg/kg) and ataxia was measured for 60 minutes. Average ataxia scores were significantly higher in MAM-E15 relative to both MAM-E17 and CON rats. There were no differences between MAM-E17 and CON in baseline or PCP-induced ataxia. **(B)** Motor activation (progressive score from movement to locomotion to stereotypy) displayed during the same testing period described for panel A. $^{\#}p < .05$ relative to MAM-E17 and CON; *MAM-E15, MAM-E17 > CON, $p < .05$; %main effect of PCP, $p < .05$. CON, control; MAM, methylazoxymethanol acetate; PCP, phencyclidine.

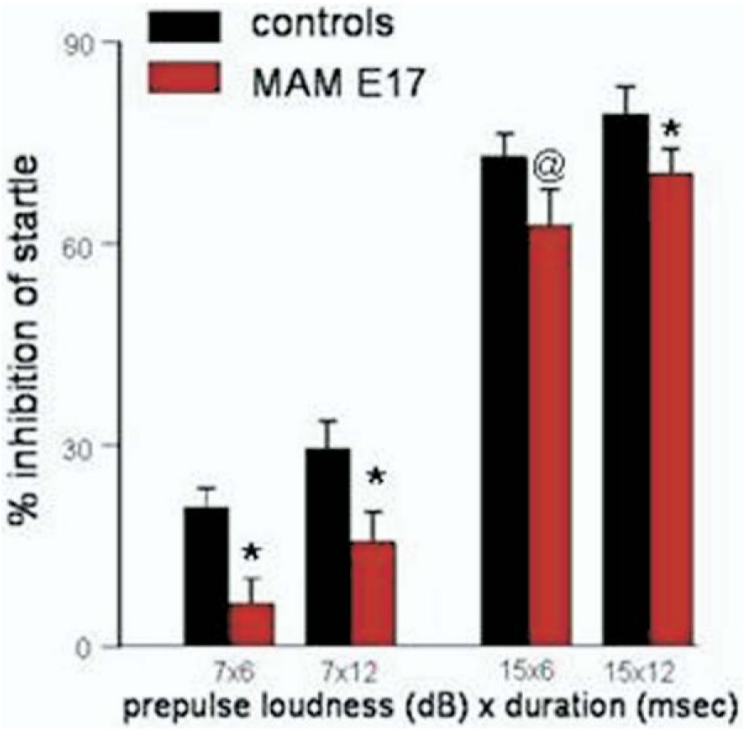

Figure 8.
Prepulse inhibition of the acoustic startle reflex. Startle tones and prepulse tones consisted of white noise bursts delivered above a background of 55 dB. Startle tones were 100 dB/40 milliseconds. The intertrial interval was 15 ± 6 seconds. $^{*}p < .05$, $^{@}p < .1$ relative to control rats.

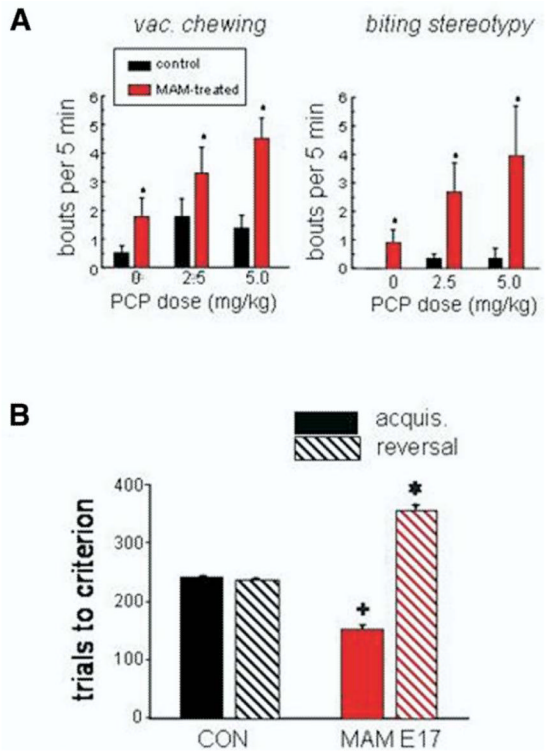

Figure 9.

Spontaneous and learned behaviors mediated by the frontal cortex in the adult offspring of dams injected on E17 with saline (CON; black bars) or MAM (MAM-E17, red bars). **(A)** Orofacial dyskinesias. Vacuous chewing (left panel) and biting stereotypy (right panel) following injection of vehicle (dose = 0) or phencyclidine (PCP 2.5, 5.0 mg/kg, IP). *increased baseline expression and greater effect of PCP in MAM-E17 rats ($p < .05$, gestational treatment × PCP interaction). **(B)** Reversal learning. Acquisition of the initial discrimination (acquisition, solid bars) was significantly faster in MAM-E17 rats. However, MAM-E17 rats required significantly more trials to learn the reversal of the discrimination (stippled bars). $^{+}p < .05$ compared with acquisition in control rats; $*p < .05$ compared with reversal in control rats. CON, control; MAM, methylazoxymethanol acetate; PCP, phencyclidine; IP, intraperitoneal.

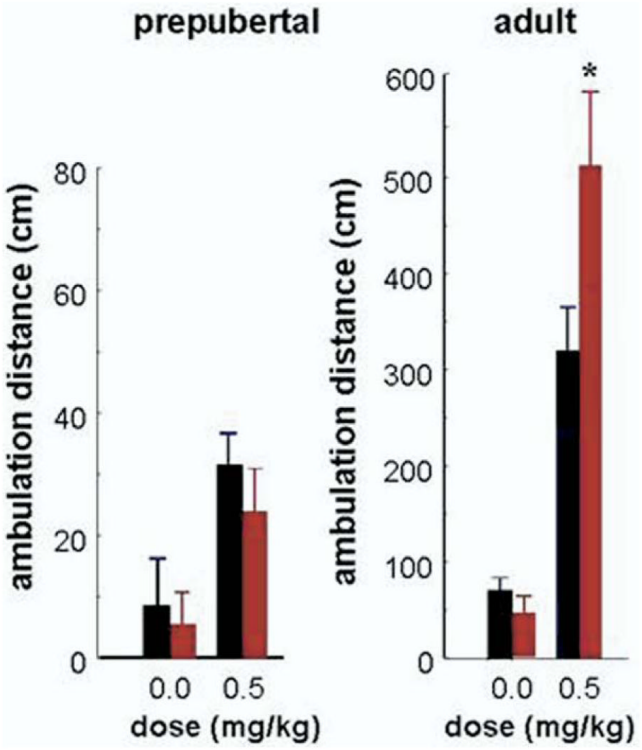

Figure 10.

Ambulation following administration of saline or amphetamine (.5 mg/kg, IP) in prepubertal (tested between P35–P40; left panel) and adult (right panel) offspring. There were no differences in ambulation between control offspring (black bars) and MAM-E17 offspring (dark red bars) tested prepubertally. However, as adults, MAM-E17 rats show a significantly increased response to amphetamine. *amphetamine-saline difference, $p < .05$ relative to control rats tested as adults. IP, intraperitoneal; MAM, methylazoxymethanol acetate.

Table 1

Membrane Properties of PFC Neurons in CON and MAM-E17 Rats

Experimental Group	RMP (mV)	Input Resistance (MΩ)	Spike Threshold (mV)	Spike Threshold (mV)
CON	−68.4 ± 1.3	21.4 ± 2.5	−46.2 ± 2.3	21.1 ± 2.2
MAM-E17	−62.1 ± 1.5[a]	30.0 ± 2.9[a]	−39.0 ± 2.7[a]	20.7 ± 2.3

PFC, prefrontal cortex; CON, control; MAM, methylazoxymethanol acetate; RMP, resting membrane potential.

[a]two-tailed Independent *t* test, $p < .05$, MAM-E17 versus CON.

Biol Psychiatry. Author manuscript; available in PMC 2012 July 13.

Table 2

Comparison of Neuroanatomical Characteristics Reported in Schizophrenia Patients with Present Findings in the MAM-E17 Model

Imaging or Neuropathological Findings in Schizophrenia	References	Present Findings in MAM-E17 Model
Reduction in tissue volume or thickness Reliability/severity: Hippocampus/parahippocampal region > frontal lobe > parietal or lateral frontal	Harrison 1999 Selemon et al 2003 Wright et al 2000	Reduced cortical thickness or area significant in HIPP, parahippocampal cortex, and mPFC but not in frontoparietal
Correlations between reduction in hippocampal volume and size and/or function of frontal lobe	Wible et al 1995 Bilder et al 1995	HIPP size correlates with PFC thickness and degree of orofacial dyskinesia
Selective reduction of size and/or cell number in anterior/medial dorsal thalamus	Ananth et al 2002 Thune and Pakkenberg 2000	Reduced size of medial dorsal thalamus but not medial geniculate body
Increased neuron packing density in dorsal frontal cortex (Brodmann area 9) and occipital cortex but not in ventrolateral frontal cortex (Brodmann area 45)	Selemon et al 1995, 2003	Increased neuron packing density in mPFC and OCC but not frontoparietal cortex
No difference in neocortical neuron number	Thune and Pakkenberg 2000	No difference in neocortical neuron number

MAM, methylazoxymethanol acetate; mPFC, medial prefrontal cortex; HIPP, hippocampus; PFC, prefrontal cortex; OCC, occipital.

Biol Psychiatry. Author manuscript; available in PMC 2012 July 13.